GEOPHYSICAL RESEARCH LETTERS, VOL. 40, 123–127, doi:10.1029/2012GL054315, 2013

Toward quantifying discrete groundwater discharge from frozen seepage faces using thermal infrared images

Priyanka Pandey,[1] Tom Gleeson,[2] and Michel Baraer[3]

Received 22 October 2012; revised 21 October 2012; accepted 25 November 2012; published 16 January 2013.

[1] Frozen groundwater seeps from discrete features, such as fractures and faults, are common along steep faces of cliffs, mines, quarries, and road cuts in cold environments at high elevations and latitudes. Our objective is to test whether thermal infrared imaging can be used to quantify groundwater discharge from such discrete features in freezing conditions. Discrete seeps and freezing cliff faces were simulated in a cold room laboratory with a systematic series of experiments captured through infrared imaging. Two zones of distinct surface temperatures were observed at the ice surface: a zone of relatively warm and constant surface temperature above a zone with high thermal gradients. Experimental conditions impacted the length of the relative warm zone. A strong correlation is observed between length of the relative warm zone and the discharge rate suggesting that groundwater discharge from discrete features could be quantified using noninvasive infrared imaging. **Citation:** Pandey, P., T. Gleeson, and M. Baraer (2013), Toward quantifying discrete groundwater discharge from frozen seepage faces using thermal infrared images, *Geophys. Res. Lett.*, *40*, 123–127, doi:10.1029/2012GL054315.

1. Introduction

[2] Groundwater fluxes are hard to quantify [*Winter et al*., 1998], except at the watershed scale where they are often quantified as base flow [*Arnold et al*., 1995; *Szilagyi et al*., 2003]. Groundwater is increasingly being recognized as playing a key role in cold-region hydrology at high latitudes [*Rouse*, 2000; *Smith et al*., 2007] and high altitudes [*Baraer*, 2009]. In these environments, fluxes of groundwater may increase with the changing climate as permafrost melts and degrades [*Bense et al*., 2009; *Ge et al.*, 2011; *Zhenniang et al*., 1993]. Therefore, new methods for quantifying small-scale groundwater fluxes in cold regions are crucial.

[3] Temperature has been exploited as a hydrologic tracer since the 1960s in part because groundwater has a smaller intra-annual temperature amplitude than surface water or the land surface [*Anderson*, 2005]. The recent developments of relatively low-cost temperature sensing equipment such as ibutton® [*Johnson et al*., 2005], distributed fiber optic cables [*Westhoff et al*., 2007], and affordable thermal imagery provide new opportunities to further develop temperature as a hydrologic tracer. Recently, ground-based thermal infrared imaging has been used to qualitatively locate large groundwater springs and characterize diffuse seepage faces with variable groundwater discharge flux [*Loheide and Gorelick*, 2006; *Pfister et al*., 2010; *Waldick and Conant*, 2006]. For example, *Deitchman and Loheide* [2009] analyzed seepage faces on opposing stream banks to demonstrate that thermal infrared imaging could detect unsaturated and saturated zones and that groundwater flow is more discrete and heterogeneous than commonly modeled and conceptualized. Thermal infrared imaging has also been used to detect and quantify the localized groundwater inflows into small streams using a simple thermal mixing model [*Schuetz and Weiler*, 2011]. *Pfister et al*. [2010] conducted experiments using ground-based infrared imagery and proved that it can be used to discriminate areas with snow cover, snow melt, soil seepage, and stream water in a hill slope-riparian-stream system. Despite the progress of these previous studies, directly estimating groundwater fluxes from thermal imagery without the use of heat budgets or thermal mixing models has not previously been possible.

[4] Our objective is to test whether passive thermal infrared imaging could be used in cold environments to directly quantify groundwater discharge flux without relying on mixing or heat budget models. Groundwater seeps from discrete features such as fractures and faults play important roles in sliding failure [*Gentier*, 2005], stream bank erosion [*Midgley et al*., 2012], or river contamination [*Tesoriero et al*., 2009], and are common along cliffs, mines, quarries, and road cuts. Figures 1a and 1b exemplify such a hydrologic setting, where thermal infrared imaging has been used to capture temperature distribution across the width and height of frozen seep. At a very high flow rate, groundwater may not appreciably cool as it runs down the cliff face, whereas at a very low flow rate, the seeps may freeze and be blocked. Between these two end members, we hypothesized that the rate of groundwater cooling observed on ice using a thermal image, is a function of the discharge rate if all other conditions (temperature, radiation, wind speed, humidity, etc.) are constant. We tested this hypothesis using experiments in a cold room laboratory. Variables that were considered include discharge rate, ambient temperature, slope, and friction of the freezing surface and wind velocity.

2. Methodology

[5] Thermal images were captured every 15 min of an experimental setup placed inside a computer-controlled cold room with –5°C temperatures for most experiments (Figure S1

All Supporting Information may be found in the online version of this article.

[1]Department of Bioresource Engineering, McGill University, Montréal, Quebec, Canada.
[2]Department of Civil Engineering, McGill University, Montréal, Quebec, Canada.
[3]Department of Construction Engineering, École de Technologie Supérieure, Université du Québec, Montréal, Quebec, Canada.

Corresponding author: T. Gleeson, Department of Civil Engineering, McGill University, 817 Sherbrooke Street West, Montréal, Quebec H3A 0C3, Canada. (tom.gleeson@mcgill.ca)

0094-8276/13/2012GL054315

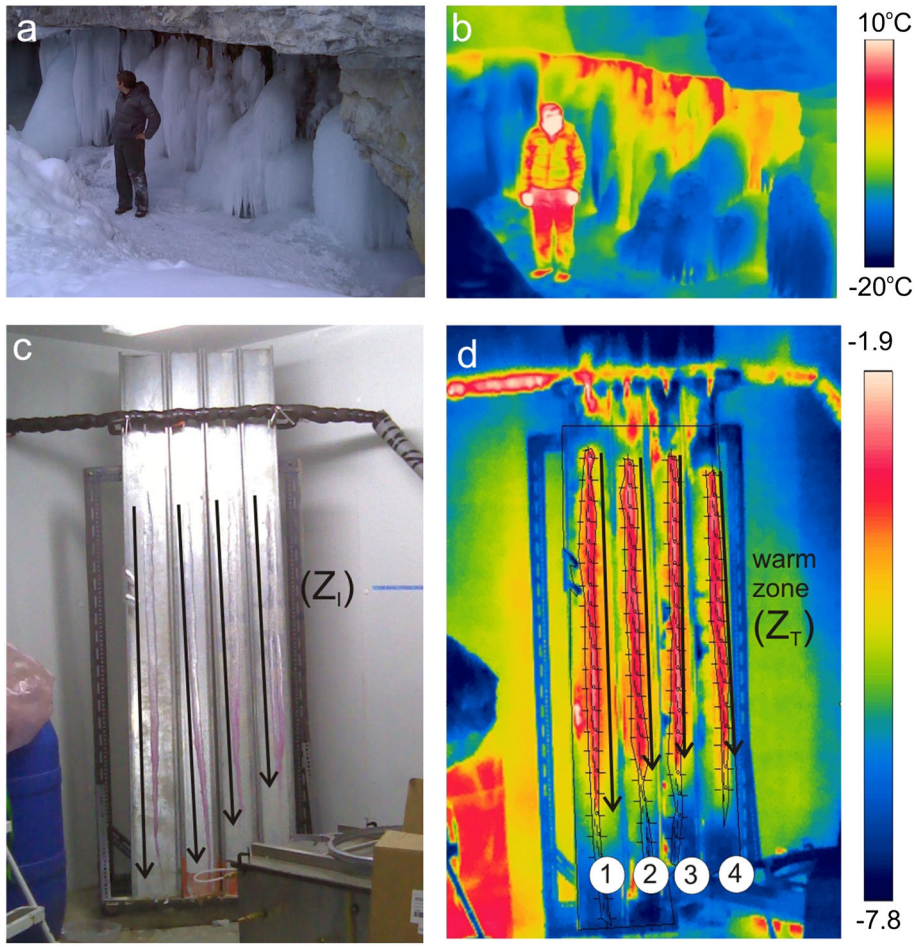

Figure 1. (a) Digital image example of a frozen groundwater seep in the Canadian Rockies; (b) corresponding thermal image of frozen groundwater seep; (c) digital image of the experimental setup in a cold room showing the ice surface length, Z_I; (d) thermal image of experimental setup showing spot meter temperature analysis tools placed across the length of ice formations, red indicating length of the relatively warm zone Z_T, and dark blue representing cooler sections on ice below.

of Supporting Information). A ~10°C water source placed outside a cold room fed four hypodermic needles that represent the groundwater seeps. The water dripped from the needles onto an inclined metal surfaces representing a cliff (Figures 1c and 1d). Few drops of phenolphthalein were added to the water source to make the ice visible distinctly against the metal sheet surface. Seeps were separated onto different metal surfaces so that they did not interact thermally or hydraulically. A series of experiments were completed to develop relationships between the temperature variations as observed in a thermal infrared image and the slope and friction of the surface on which the water freezes and the flow rate at which the water is being pumped. Each experiment was run until the thermal infrared imaging was stabilized in successive images (generally after 3–4 h). The experimental conditions chosen for the base case scenario were 1.5 mL/min pumping rate from each of the syringes, no wind and metal sheets that are inclined at 73° with sand glued to the surface to increase friction (Table S1). Parameters were systematically and individually varied from this base case scenario. An additional 15 h test was conducted to examine the longer term development of the frozen seeps. During all experiments the temperature of the water source and of the water near the hypodermic needles as well as the temperature and humidity of the cold room were recorded using ibutton® DS1922L and a Lascar® EL-USB-2-LCD data logger with an accuracy of ±0.5°C and ±0.3°C, respectively. The dimensions of the frozen seeps and the volume of water that flowed down without freezing were measured using containers placed at the bottom of the setup, throughout the experiments.

[6] Thermal and digital photos were collected from a distance of 510 cm using a FLIR Systems (North Billerica, MA) B300 thermal infrared camera, which measures surface temperature using a 320 × 240 focal plane array with a spectral range of 7.5–13 μm, with ±2% or 2°C accuracy for absolute temperatures. The sensitivity for relative temperature, the noise equivalent temperature difference [*Shea et al.*, 2012] is 0.05°C, which makes the relative temperature measurements around 40 times more accurate than the absolute measurements. We therefore used relative temperature, ΔT, the difference between the temperature at a given point of the ice surface and the temperature measured at the top of this ice surface (Figure 2a) for the interpretation of the infrared thermal images. Thermal images were corrected for emissivity, air temperature, and relative humidity. We assumed a uniform local emissivity of 0.96 based on emissivity values of water for smooth ice [*Karev et al.*, 2007; *Lingen et al.*, 2003]. Relative temperatures were systematically computed at different elevations (Z) at 8 cm intervals,

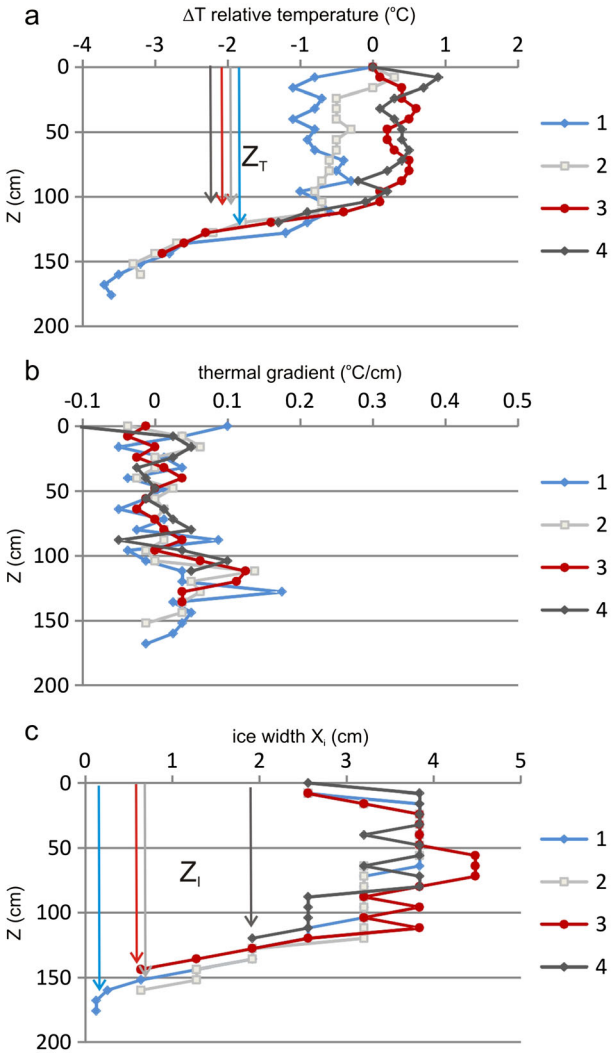

Figure 2. Base case scenario ice growth characteristics measured at the end of the experiment: (a) relative temperature; (b) thermal gradient, and (c) horizontal width of ice growth. Z represents the measured distance from the upper point of the ice formation and numbers 1, 2, 3, and 4 represent the sheet numbers as shown in Figure 1.

using the spotmeter tool in the software ThermaCAM Research Professional 2.10 (Figure 1d). The experimental setup led to a small range of observation angles so the impact of the observation angle variations on the ice and water emissivity was negligible.

3. Results

[7] Thermal images of experiments show two distinct thermal zones across the ice length. The upper zone, that usually covers more than half of the total ice surface is characterized by a relatively uniform surface temperature that differs from the top part of the ice formation by –1 to +1°C only. This "warm" thermal zone, which appears in red on the thermal images (Figure 1d), is followed by a zone of decreasing ice surface temperature, which varies in color from red at the top to blue at its lower extremity. When compared to the digital picture of the same ice formation (Figure 1c) the thermal image shows that the zone of decreasing temperature superimposes, at least partly, the area of narrowing of the ice formation width, suggesting possible related phenomenon. Visual observations made during the experiments indicate that the warmer section of ice is wetter than the cooler one.

[8] To characterize the warm thermal zone of each experiment, we introduce Z_T the vertical length of the zone of relatively warm and constant in temperature (Figure 2a). Z_T is determined from a breakpoint analysis using segmented regressions. For each experiment, a series of linear regressions are made using consecutive calculations of thermal gradient (ΔT) at different elevations (Z). Coefficients of determinations R^2 are calculated for all segments of the ice formation that start at its top and are longer than half of the warm zone. The breakpoint is defined as being the intersection of the regression line through the relatively warm zone and a line connecting two consecutive points with the highest thermal gradient. The breakpoint is thus the top of the zone of high thermal gradients (Figure 2b). For each experiment, the comparison between Z_T, the extent of the warm zone in ice formations and X_i, the horizontal width of ice growth (Figure 2c) is made and Z_I, the ice surface length measured on the corresponding digital picture, is also represented. The horizontal width of ice growth (X_i) highlights the elevations where significant ice growth occurs.

[9] Resulting from the sensitivity analysis, Figure 3 (and additional data in Figures S2, S3, S4, and S5 of the Supporting Information) shows to what degree three of the different experimental parameters influence Z_T and Z_I. First, Figure 3 shows that Z_T and Z_I vary logarithmically with the dripping water flow rate. With a robust regression coefficient of determination of 0.89, Z_T is the parameter that correlates the best with the flow rate. This relation suggests that, wherever the other key parameters do not vary, Z_T represents a proxy for seeping flow rate. The wind influence on Z_T is different to that of flow rate (Figure S5a). As the wind velocity increases compared to the base scenario, we see the vertical extent of the ice formation decreasing. This effect is not linear and seems to stabilize for wind speed over 1 m/s. Finally, Figure S3c shows that the effect of an increase of the slope leads to an increase in the Z_T value. In general, Figures 3 and S5 show that the relation between Z_T and the studied variables is more consistent than the one observed with Z_I. Results from other experiments do not contradict nor add significantly to what is shown in Figure 3 so they are shown as Supporting Information. Z_T varied during the longer experiment due to experimental conditions that were harder to keep constant for longer duration (Figure S6).

4. Discussion

[10] The analysis of the infrared pictures taken during the experiments reveals the existence of two distinct thermal zones in the studied ice formation: a relatively warm zone in the upper ice formation above a zone characterized by a higher thermal gradient. The exact mechanisms that make these two zones are not fully identified yet. Different models of wet growth of ice present the ice/water interface as a layer of critical importance for the ice formation layer [*Blackmore et al.*, 2002; *Makkonen*, 2012]. This interface is often described as a mix of ice and water that is overlaid by a liquid water film that moves downward and that keeps supplying liquid to the system [*Gagnon and Paquette*, 2011]. This

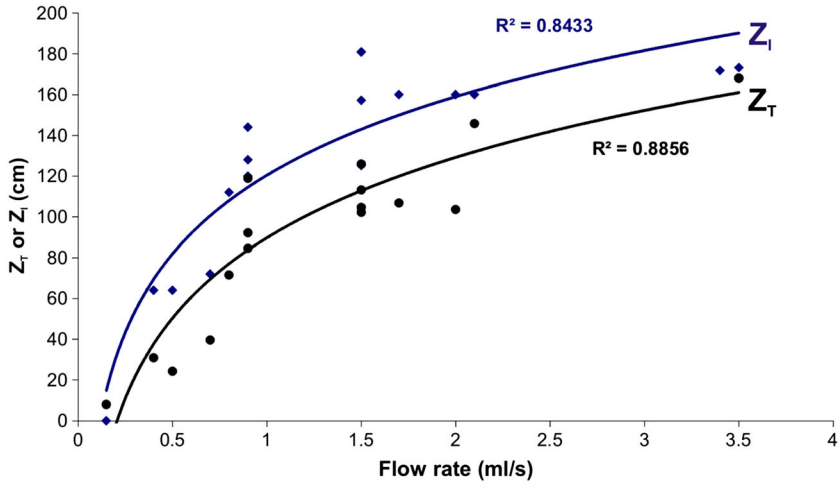

Figure 3. Relationship between Z_I and Z_T with flow rate. The blue squares represent $Z_{I,}$ and the black diamonds represent Z_T.

model implies that the entire heat transfer from the ice forming layer to its environments is provided from the change of phase. In our experimental conditions, these ice forming conditions are observed at the upper part of the ice formation. Because infrared cameras capture the temperature of a very thin film of several tens of micrometers for water [*Horwitz*, 1999; *McDonald*, 1960], it can be hypothesized that the warm zone we systematically observe in our experiment is the liquid water film surface that overlay the ice/water interface.

[11] As the liquid water flows down the inclined plan, part of it gets trapped at the ice/water interface making the water film thinner or intermittent with the increasing distance from the top of the ice formation. The model of uniform wet ice growth described above therefore stops being applicable at a given distance from the top of the ice formation. The ice/water interface does not receive enough liquid water to sustain ice growth and part of the heat transfer becomes available to remove the sensible heat of the water. The resulting surface cooling could correspond to the second thermal zone observed through the infrared camera. Although this scenario links thermography results with heat and matter exchange models, further work is needed to confirm its relevance.

[12] The result of the sensitivity analysis presented here suggests that using the vertical extent of the warm zone in the ice formation Z_T would be more appropriate than using the ice formation length calculated from digital photos to characterize ice formation from seeping water in subfreezing environments. For each studied experimental variable the parameter Z_T exhibits relationships with the variable that are stronger than those obtained using Z_I. Additionally, the ice length integrates a longer term average flow rates whereas Z_T represents the water flux at the time of imagery more accurately.

[13] Where all other parameters are stable (air temperature, wind, etc.) Z_T might be used for evaluating the seepage flow rate from natural ice formations. The strong logarithmic correlation that was observed between the seeping flow rate and Z_T in our experimental condition could serve as a base for future research in this area. Frozen seeps in the natural environment are complex, rapidly changing, and have a different thermal conductivity and friction than the experimental conditions, which must all be considered in future research. But our results provide a first step toward quantifying groundwater discharge rates using thermal imagery alone.

5. Conclusions

[14] The systematic presence of two distinct thermal zones at the surface of the ice formations produced in controlled conditions made possible establishing a strong relationship between Z_T, the length of the warm zone and the flow rate of the seeping water. This makes passive thermal infrared imaging a potential technique to directly quantify groundwater discharge flux in cold environments without relying on mixing models or heat budget models. Because other experimental parameters such as wind speed or inclined surface slope also influence Z_T, studying the combined effects of all these key parameters should represent a step in the direction of establishing a protocol for the use of that method in the natural environment. Adaptation to the natural environment will also require taking into account parameters that may impact the interpretation of thermal images such as direct solar illumination, reflected radiations, friction, and environmental heterogeneity.

[15] Our results suggest that for the first time, to our best knowledge, discrete groundwater discharge could be quantified directly and noninvasively, without thermal or mixing models. For hydrologic systems in cold environments, we here provide a new means for quantifying groundwater discharge for the relatively limited range of environmental conditions we tested where water would discharge at a relatively low flow rate to a conductive surface in –5°C air temperatures. However, with limited studies, the application conditions of the method we propose could be considerably enlarged for a broader application in natural conditions including, but not limited to, environments with colder air temperatures, winds, or higher cliffs with undulating surfaces. An important first step may be north-facing surfaces that are relatively protected from the wind and solar radiation. Even in conditions where groundwater may not appreciably cool as it runs down the cliff face (high flow rates) or where the seeps may freeze and be blocked (low flow rates), our method could be useful because it would give a maximum or minimum groundwater

discharge rate, respectively. These possibilities make our method of potential use in cold region mines, quarries, and cliffs. Fundamentally, we show the potential for quantifying fluxes from discrete thermal signal warm or cool in the environment. Similar methods could be developed for how cool groundwater discharge from a discrete feature warms and evaporates during the summer. The new method is based on discrete thermal signals that are different than ambient conditions, and have a surface to cool or warm over. Therefore, our results could motivate further studies that could transform how we quantify discrete groundwater discharge in diverse environments, and how we interpret discrete thermal signals in hydrothermal and volcanic environments.

[16] **Acknowledgment.** The authors acknowledge J. Bartczak, W. Cook, and S. Ghoshal for assistance with lab work and experimental setup, and two anonymous reviewers for constructive comments on this manuscript.

References

Anderson, M. P. (2005), Heat as a ground water tracer, *Ground Water*, *43*(6), 951–968.

Arnold, J. G., P. M. Allen, R. Muttiah, and G. Bernhardt (1995), Automated base flow separation and recession analysis techniques, *Ground Water*, *33*(6), 1010–1018.

Baraer, M. (2009), Characterizing contributions of glacier melt and groundwater during the dry season in a poorly gauged catchment of the Cordillera Blanca (Peru), *Adv. Geosci.*, *22*, 41.

Bense, V. F., G. Ferguson, and H. Kooi (2009), Evolution of shallow groundwater flow systems in areas of degrading permafrost, *Geophys. Res. Lett.*, *36*(22), L22401.

Blackmore, R. Z., L. Makkonen, and E. P. Lozowski (2002), A new model of spongy icing from first principles, *J. Geophys. Res.*, *107*(21), 9-1-9-15.

Deitchman, R. S., and S. P. Loheide II (2009), Ground-based thermal imaging of groundwater flow processes at the seepage face, *Geophys. Res. Lett.*, *36*(14), L14401.

Gagnon, J., and E. Paquette (2011), Procedural and interactive icicle modeling, *Visual Computer*, *27*(6–8), 451–461.

Ge, S., J. McKenzie, C. Voss, and Q. Wu (2011), Exchange of groundwater and surface-water mediated by permafrost response to seasonal and long term air temperature variation, *Geophys. Res. Lett.*, *38*(14), L14402.

Gentier, S. (2005), Analysis of sliding failure of the Viviers-Basques' (France) jointed rock cliff, paper presented at Impact of Human Activity on the Geological Environment EUROCK 2005: Proceedings of the International Symposium EUROCK 2005, 18-20 May 2005, Brno, Czech Republic, p. 63. Taylor and Francis.

Horwitz, J. W. (1999), Water at the Ice Point: A useful quasi-blackbody infrared calibration source-erratum, *Appl. Opt.*, *38*(31), 6564–6564.

Johnson, A. N., B. R. Boer, W. W. Woessner, J. A. Stanford, G. C. Poole, S. A. Thomas, and S. J. O'Daniel (2005), Evaluation of an inexpensive small-diameter temperature logger for documenting ground water–river interactions, *Ground Water Monit. Rem.*, *25*(4), 68–74.

Karev, A. R., M. Farzaneh, and L. E. Kollár (2007), Measuring temperature of the ice surface during its formation by using infrared instrumentation, *Int. J. Heat Mass Transfer*, *50*(3–4), 566–579.

Lingen, B., G. Zhiqiu, L. Longhua, Z. Yabin, C. Roger, and X. Zhang (2003), Observational estimation of heat budgets on drifting ice and open water over the Arctic Ocean, *Science in China Series D: Earth Sciences*, *46*(6), 580–591.

Loheide, S. P., and S. M. Gorelick (2006), Quantifying stream – aquifer interactions through the analysis of remotely sensed thermographic profiles and in situ temperature histories, *Environ. Sci. Technol.*, *40*(10), 3336–3341.

Makkonen, L. (2012), Ice adhesion - Theory, measurements and countermeasures, *J. Adhesion Sci. Technol.*, *26*(4-5), 413–445.

McDonald, J. E. (1960), Absoption of atmospheric radiation by water films and water clouds, *J. Meteorol.*, *17*, 6.

Midgley, T. L., G. A. Fox, G. V. Wilson, D. M. Heeren, E. J. Langendoen, and A. Simon (2012), Seepage-induced streambank erosion and instability: In-situ constant-head experiments, *J. Hydrolog. Eng.*, doi:10.1061/(ASCE)HE.1943-5584.0000685.

Pfister, L., J. J. McDonnell, C. Hissler, and L. Hoffmann (2010), Ground-based thermal imagery as a simple, practical tool for mapping saturated area connectivity and dynamics, *Hydrol. Processes*, *24*(21), 3123–3132.

Rouse, W. R. (2000), The energy and water balance of high-latitude wetlands: controls and extrapolation, *Global Change Biol.*, *6*(S1), 59–68.

Schuetz, T., and M. Weiler (2011), Quantification of localized groundwater inflow into streams using ground-based infrared thermography, *Geophys. Res. Lett.*, *38*(3), L03401.

Shea, C., B. Jamieson, and K. W. Birkeland (2012), Use of a thermal imager for snow pit temperatures, *Cryosphere*, *6*(2), 12.

Smith, L. C., T. M. Pavelsky, G. M. MacDonald, A. I. Shiklomanov, and R. B. Lammers (2007), Rising minimum daily flows in northern Eurasian rivers: A growing influence of groundwater in the high-latitude hydrologic cycle, *J. Geophys. Res.*, *112*(G4), G04S47.

Szilagyi, J., F. E. Harvey, and J. F. Ayers (2003), Regional estimation of base recharge to ground water using water balance and a base-flow index, *Ground Water*, *41*(4), 504–513.

Tesoriero, A. J., J. H. Duff, D. M. Wolock, N. E. Spahr, and J. E. Almendinger (2009), Identifying pathways and processes affecting nitrate and orthophosphate inputs to streams in agricultural watersheds, *J. Environ. Qual.*, *38*(5), 1892–1900.

Waldick, M. K., and B. Conant (2006), Evaluation of land-based infrared thermography to identify and quantify groundwater discharge to a small stream., Paper 13-8, Geological Society of America Annual Meeting and Exposition, 22–25 October, Philadelphia, Pennsylvania.

Westhoff, M. C., H. H. G. Savenije, W. M. J. Luxemburg, G. Stelling, N. Van De Giesen, J. Selker, L. Pfister, and S. Uhlenbrook (2007), A distributed stream temperature model using high resolution temperature observations, *Hydrol. Earth Syst. Sci.*, *11*(4), 1469–1480.

Winter, T. C., J. W. Harvey, O. L. Franke, and W. M. Alley (1998), Ground water and surface water: a single resource, *U.S. Geol. Surv. Circ. 1139*, 79.

Yang Z., F. Liang, Z. Yang, and Q. Wang (1993), The effect of water and heat on hydrological processes of a high alpine permafrost area, in *Snow and Ice Covers: Interactions with the Atmosphere and Ecosystems*, edited by H. G. Jones and T. D. Davies, p. 259, IAHS Publication No. 223.